Journal of Power Sources 193 (2009) 730–738

Contents lists available at ScienceDirect

Journal of Power Sources

journal homepage: www.elsevier.com/locate/jpowsour

Interactions of nickel/zirconia solid oxide fuel cell anodes with coal gas containing arsenic

C.A. Coyle, O.A. Marina, E.C. Thomsen, D.J. Edwards, C.D. Cramer, G.W. Coffey, L.R. Pederson*

Pacific Northwest National Laboratory, Richland, WA 99352, USA

ARTICLE INFO

Article history:
Received 14 March 2009
Received in revised form 18 April 2009
Accepted 20 April 2009
Available online 3 May 2009

Keywords:
Coal gas
SOFC
Arsenic
Nickel
Anode
Degradation

ABSTRACT

The performance of anode-supported and electrolyte-supported solid oxide fuel cells was investigated in synthetic coal gas containing 0–10 ppm arsenic at 700–800 °C. Arsenic was found to interact strongly with nickel, resulting in the formation of nickel–arsenic solid solution, Ni_5As_2 and $Ni_{11}As_8$, depending on temperature, arsenic concentration, and reaction time. For anode-supported cells, loss of electrical connectivity in the anode support was the principal mode of degradation, as nickel was converted to nickel arsenide phases that migrated to the surface to form large grains. Cell failure occurred well before the entire anode was converted to nickel arsenide, and followed a reciprocal square root of arsenic partial pressure dependence that is consistent with a diffusion-based rate-limiting step. Failure occurred more quickly with electrolyte-supported cells, which have a substantially smaller nickel inventory. For these cells, time to failure varied linearly with the reciprocal arsenic concentration. Failure occurred when arsenic reached the anode/electrolyte interface, though agglomeration of nickel reaction products may have also contributed. Test performed with nickel/zirconia coupons showed that arsenic was essentially completely captured in a narrow band near the fuel gas inlet. Arsenic concentrations of ~10 ppb or less are estimated to result in acceptable rates of fuel cell degradation.

1. Introduction

Solid oxide fuel cell (SOFC) systems have been estimated to operate at greater than 50% efficiency (higher heating value) when fueled with gasified coal, even with carbon sequestration [1–4]. Coal, however, contains multiple minor and trace components that could impact fuel cell performance, of which antimony, arsenic, cadmium, lead, mercury, phosphorus, selenium and sulfur are among those identified to be of concern because of their tendency to partition between solid and gas phases under conditions typical of warm-gas cleanup [5]. Arsenic is of particular interest, given that it is widely distributed in coals, readily forms arsine (AsH_3) and other volatile species during gasification, and is expected to be present in concentrations ranging from 0.15 to 0.60 ppmv in coal syngas [5–8].

Arsenic is a well-known poison for nickel steam reforming catalysts. The presence of 1 ppm of As_2O_3 in the steam led to irreversible degradation, and the catalysts continued to be poisoned even if arsenic was only present on the reactor walls [9]. Arsenic is known to inhibit ethane dissociation as well as hydrogen adsorption on nickel catalysts [10,11]. Arsenic also is known to poison methanol synthesis catalysts [12]. Formation of the solid phase Ni_5As_2 has been reported when nickel-based steam reforming catalysts were exposed to arsenic volatilized from arsenic oxide [13].

Several previous studies have considered the effect of arsine in coal gas on SOFC performance [14–17]. Trembly et al. observed little electrochemical degradation for arsine concentrations less than or equal to 2 ppm during ~100 h tests, and no alteration phases of nickel were found [14]. After ~800 h at 800 °C in synthetic coal gas with 0.1 ppm arsine, formation of a small quantity of the solid phase NiAs on the outer surface of the anode was reported, although electrochemical performance minimally affected [14]. Limited electrochemical consequences of short-term arsine exposure was found by Marina et al., despite extensive formation of the alteration phase Ni_5As_2 on the outer surface of the anode [15,16]. Krishnan similarly showed negligible electrochemical degradation due to arsenic exposure, and reported extensive nickel–arsenic interactions [17].

In the present study, the effect of exposure of the nickel anode to arsenic in coal gas was investigated using both electrolyte-supported and anode-supported cell designs. Electrolyte-supported cells provide more rapid response to the presence of coal gas contaminants because of a smaller nickel inventory, while anode-supported cells more closely match cell architectures being considered for large planar systems. Reaction times were extended to enable loss in electrochemical performance to be observed. In addition, coupons composed of porous

* Corresponding author at: Pacific Northwest National Laboratory, Energy & Environment Directorate, 902 Battelle Blvd, PO Box 999, Richland, WA 99352, USA. Tel.: +1 509 375 2731; fax: +1 509 375 2167.
E-mail address: larry.pederson@pnl.gov (L.R. Pederson).

0378-7753/$ – see front matter © 2009 Elsevier B.V. All rights reserved.
doi:10.1016/j.jpowsour.2009.04.042

nickel/yttria-stabilized zirconia (Ni/YSZ) anode support material were subjected to coal gas containing arsenic in both flow-through and flow-by arrangements, as a means of assessing the kinetics of arsenic–nickel interactions. Post-test analyses were performed to identify reaction products formed and their distribution. These observations were compared to the appearance of alteration phases expected from thermochemical considerations. The ultimate purpose of this work is to establish maximum permissible concentrations for arsenic and other contaminants in coal gas, to be used with large SOFC systems. This information is needed to aid in the selection of appropriate coal gas clean-up technologies.

2. Experimental

2.1. Button cell configurations

Both electrolyte-supported and anode-supported cells were used in this study. With electrolyte-supported cells, substantially less time was required for arsenic to reach the anode/electrolyte interface and to show changes in performance than anode-supported cells. Anode-supported cells enabled the effects of nickel–arsenic interactions away from the active interface to be addressed, including loss of electrical percolation.

Anode-supported button cells with an active area of 2 cm^2 were fabricated as described previously [15]. The Ni/YSZ support was approximately 1 mm thick and was comprised of a Ni/YSZ bulk layer with a 40/60 vol.% solids ratio and approximately 30 vol.% porosity. The active anode was approximately 10 μm in thickness and consisted of Ni/YSZ in a 50/50 vol.% solids ratio and 30 vol.% porosity. The electrolyte was 8YSZ (yttria-stabilized zirconia with 8 mol.% yttria), approximately 8 mm in thickness. A 4 μm thick samaria-doped ceria (SDC) barrier layer was applied to the pre-sintered at 1375 °C anode–electrolyte structure by screen printing followed by sintering at 1200 °C. A 30–50 μm thick $(La_{0.80}Sr_{0.20})_{0.98}MnO_3$ (LSM-20) cathode was applied in the same manner and sintered at 1100 °C for 2 h. The anode current collector, comprised of nickel mesh, was embedded in NiO paste and co-fired with the ceria. The cathode current collector was silver mesh embedded in LSM. Cells were sealed to alumina test fixtures with a barium aluminosilicate glass by heating to 850 °C in air. Eight cells were configured in a single box furnace, each of which had independent control of anode gases. The Ni/YSZ anode was reduced *in situ* at 800 °C by moist hydrogen saturated with water at room temperature (ca. 3% H_2O).

As a result of initial tests, it was concluded that platinum current-collecting wires were not usable in the presence of arsenic. Platinum vaporized and segregated on the Ni current collector surface, ending in complete electrical contact failure. Thick alumel and nickel wires were found to be more suitable for such environments, though partially scavenged contaminants of interest before reaching the anode. To decrease the interactions between the wire and contaminants, alumel wires were enclosed into a 2-bore alumina tube, with only an exposed wire loop touching the nickel mesh on the current collector. The exposed wire was partially coated with a barium aluminosilicate glass to limit the unwanted interactions with the gas environment.

Electrolyte-supported button cells were purchased from Fuel Cell Materials, a division of NexTech Materials, Inc. These cells were comprised of an 8YSZ electrolyte of 165 ± 8 μm in thickness, with a Ni/8YSZ anode approximately 30 μm in thickness. The cathode consisted of LSM-20, with a ~2 μm gadolinia-doped cerium oxide barrier layer between the cathode and electrolyte. Electrolyte-supported button cells were 25 mm in diameter, with 1.26 cm^2 active anode and cathode areas. A nickel oxide current-collecting grid, approximately 5 μm in thickness, was screen printed onto the cells to facilitate electrical contact. Cells were sealed to alumina test fixtures with a barium aluminosilicate glass, as with anode-supported cells.

2.2. Cell testing

Cell tests were performed in the temperature range 700–800 °C. The fuel gas consisted of synthetic coal gas, created by equilibrating 55 parts by volume hydrogen with 45 parts by volume carbon dioxide over a nickel catalyst and yielding a nominal composition of $H_2/CO/CO_2/H_2O$ = 30%/23%/21%/26%, which varies with temperature. Gas equilibration was verified by gas chromatography and by comparison of measured and expected open circuit potentials. Tests were also performed to evaluate the effects of fuel utilization and current density (or overpotential). To simulate fuel compositions corresponding to high (50, 60, and 70%) fuel utilization, the coal gas composition was adjusted with an appropriate amount of oxygen, and equilibrated over a nickel catalyst. Before introduction of a specific contaminant, cells were pre-conditioned in simulated coal gas initially at 0.7 V and then at a constant current for 50–150 h to obtain a stable baseline. The cathode was supplied with essentially pure oxygen from a pressure swing adsorption unit. This approach results in a small but constant cathodic polarization contribution. Arsine from cylinder was added to the synthetic coal gas downstream of the nickel catalyst using calibrated electronic flow controllers. All tests were performed at a constant current (0.1–0.5 A cm^{-2}) to ensure that the operating conditions on the cathode are constant throughout the test duration. Arbin Instruments multichannel controllers were used to monitor electrochemical performance of the cells, as was a Solartron Model 1255/1470 Multistat test system. The latter instrument, in addition to a Solartron Model 1260/1287 instrument, was used to obtain electrochemical impedance spectra at regular time intervals for each cell. Impedance spectra provide information on whether losses in performance are due to ohmic and/or electrodic processes.

2.3. Coupon tests

Coupons composed of Ni/YSZ anode support material were exposed to coal gas containing arsine in both flow-through and flow-by configurations. In flow-through tests, porous Ni/YSZ discs without a dense electrolyte were sealed onto alumina tubes with barium aluminosilicate glass, similar to procedures used for button cells. After NiO reduction, coal gas containing 40 ppm arsine was forced to flow through the cermet coupon at a flow rate of 0.67 cm^3 gas cm^2 cross-sectional area s^{-1} in the temperature range 300–800 °C for ~75 h. The extent of reaction was assessed by electron microscopy following the tests, as described below. In flow-by tests, porous Ni/YSZ coupons 2.5 cm × 5 cm in dimension were sealed onto an alumina fixture in a configuration similar to that of a cell within a planar SOFC stack. In this case, the coupon included a dense 8 μm-thick YSZ electrolyte layer to maintain gas tightness. Coal gas containing 2 ppm arsine flowed lengthwise across the coupon. The flow rate was 3.4 cm^3 gas-cm^{-2} s^{-1} (200 cm^3 cm^{-2} min^{-1} or 200 sccm), corresponding to a fuel utilization of 50%, though these coupons were not operated electrochemically.

2.4. Post-test analyses

Following termination of electrochemical tests, surfaces and cross-sections of individual cells were analyzed using scanning electron microscopy and energy dispersive spectroscopy (SEM/EDS), providing information on whether alteration phases were formed, the depth of interaction, and the composition of the

reacted anode. X-ray mapping was used to show elemental distributions and new phase formation. Selected samples were additionally analyzed using electron backscatter diffraction (EBSD) to identify specific crystal structures of alteration products. This approach is particularly useful in distinguishing among multiple possible alteration phases that are similar in composition. The same approach was used to analyze surfaces and polished cross-sections of Ni/YSZ coupons.

3. Results

3.1. Performance of anode-supported cells

No immediate response in cell performance was observed after introduction of arsenic in synthetic coal gas, though after long-term exposure, cell power output fell abruptly depending on the arsenic concentration. Fig. 1 gives cell power for a set of anode-supported cells that were exposed at 700, 750, 800 °C to coal gas with different concentrations of AsH_3, normalized to that just prior to contaminant introduction. Typically, cells exposed to low arsine concentrations showed 0–15 mV voltage loss at low AsH_3 concentrations over 500 h, which is indistinguishable from the performance cells tested without the contaminants. No clear temperature effect in the range 700–800 °C was noticed. Times to failure decreased with increased arsenic concentrations in coal gas, with cells exposed to 10 ppm of AsH_3 failing within 100–200 h, while those exposed to 1 ppm AsH_3 surviving for 500–1000 h. Tests performed with arsine in hydrogen with 3% steam yielded results similar to those in coal gas.

Anode-supported cells were additionally tested at varied current densities (0.1–1 A cm^{-2}) with a fixed amount of AsH_3 of 1 ppm at 800 °C. No additional degradation was seen: cells operated similarly to those tested in coal gas with no arsenic at identical current densities. Another set of cells was tested at 700 and 800 °C in a coal gas with oxygen additions to simulate 50, 60, and 70% fuel utilization in the presence of 1 ppm of AsH_3. Again, no changes in rates of degradation as a function of fuel utilization were observed.

Occasionally a cell would rapidly recover to essentially the initial power output for hours or even days before failing permanently. Erratic changes in cell output after long exposure to arsenic are attributed to a loss and return of electrical connectivity in the anode support. As is discussed in later sections, arsenic reactions with nickel led to the formation of alteration phases that are accompanied by excessive grain growth. The alteration products are electrically conductive, so electrical bridges between the current collector and active anode can be temporarily restored as the nickel anode is being altered.

Electrochemical impedance spectra obtained in parallel were consistent with the results of dc tests. Fig. 2 provides typical spectra corresponding to different periods of exposure to 1 ppm of AsH_3 at 700 °C. No differences in either ohmic (high frequency x-axis intercept at left-hand side of the figure) and electrodic (difference between low and high frequency x-axis intercepts) resistances

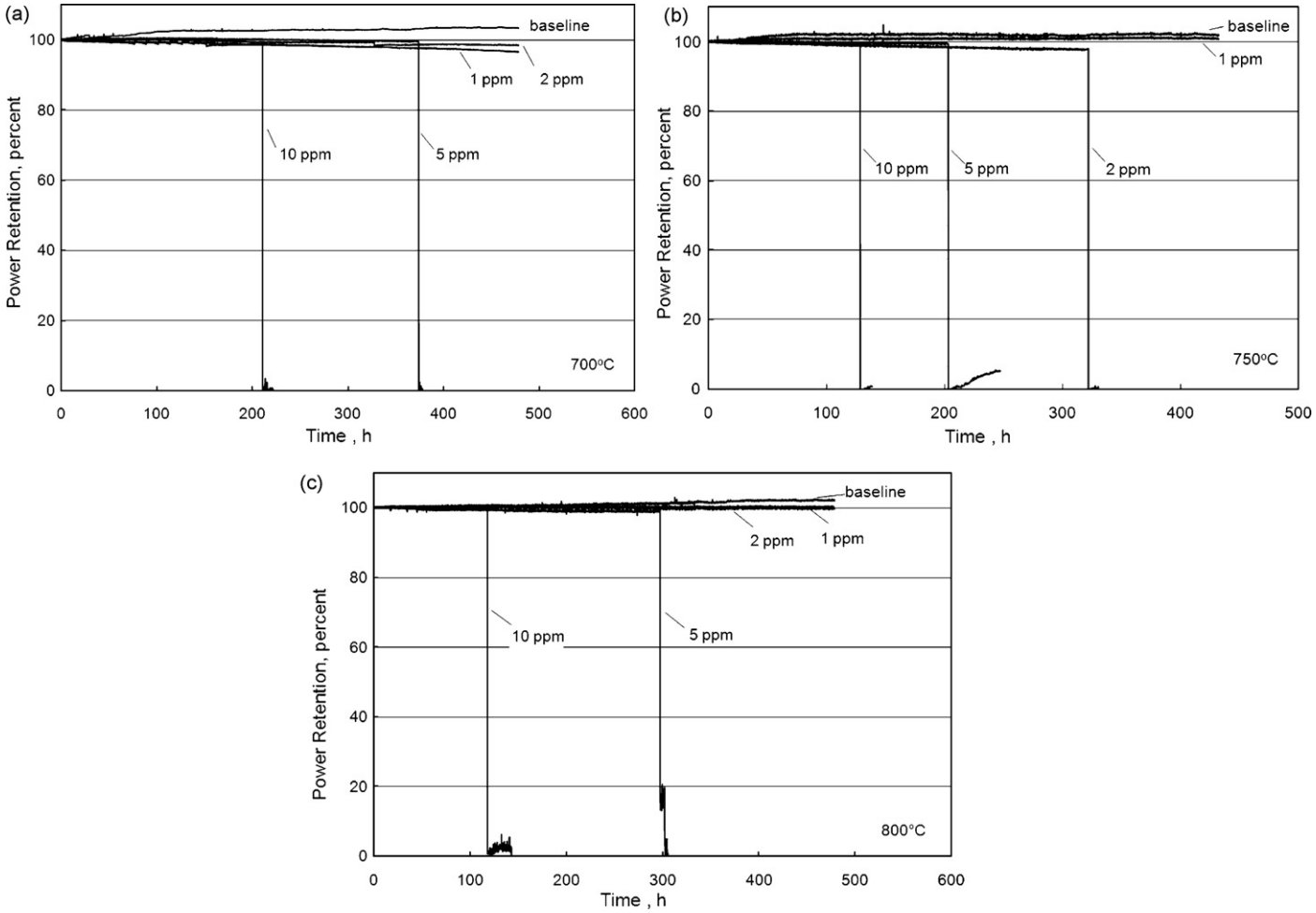

Fig. 1. Normalized cell power at constant current density (0.1 A cm^{-2}) before and after 0 (baseline), 1, 2, 5, and 10 ppm of AsH_3 introduction to coal gas at (a) 700 °C, (b) 750 °C, and (c) 800 °C. Initial cell potentials ranged from 0.86 to 0.90 V.

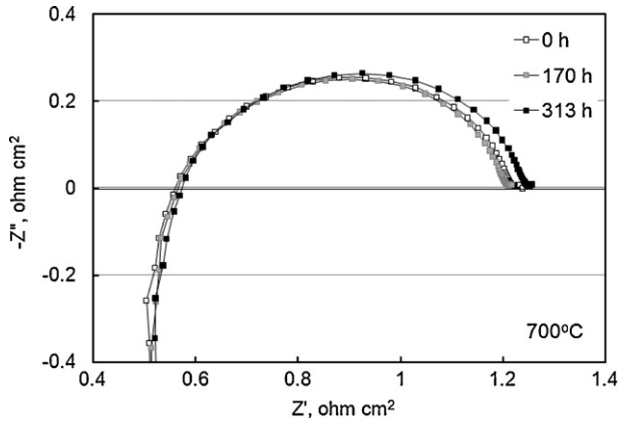

Fig. 2. Electrochemical impedance spectra obtained before (0 h) and after 170 and 313 h of exposure to 1 ppm of AsH_3 at 700 °C. Spectra were obtained with a dc bias current of 0.1 A cm^{-2}.

after relatively short <170 h exposure to arsenic were found. After 300 h of exposure, a slight increase in the ohmic component was observed, most likely due to changes in current collection in the upper part of the cell. No accompanying changes in electrodic resistances were observed, however. This behavior supports a conclusion that arsenic had not poisoned the active anode/electrolyte interface during this testing period.

At the termination of the test, cells were cooled down to room temperature in hydrogen in the absence of arsenic to prevent extraneous phases from being formed at low temperature. Detailed post-mortem SEM/EDS analyses performed both on the surface and polished cross-sections revealed partial to complete conversion of nickel into nickel arsenides. No zirconia–arsenic reactions were apparent in any tests performed in this study. Typical results are given in Fig. 3, which correspond to exposure to 1, 2, 5, and 10 ppm of AsH_3 for ~500 h at 800 °C. The depth of reaction increased with increased arsenic concentration, with extensive agglomeration and coalescence. Although nickel arsenides are electrically conductive [18], electronic percolation in the outer portion of the anode support appeared to be severely compromised by these changes. The nickel current collector and nickel mesh, if present, were also transformed into large nickel arsenide crystals. These reaction products were only very weakly bound to the Ni/YSZ anode support and often separated during the cool down procedures or during cell dismounting.

Reaction of nickel with arsenic, accompanied by diffusion and extensive coalescence of the reaction product, resulted in some regions of the anode being converted to essentially pure YSZ, nearly completely free of nickel, as illustrated in Fig. 4. However, the anode remained intact at greater depths, including the area of the active anode/electrolyte interface. If electrical contact to the active interface was maintained anywhere within the cell, electrochemical performance showed little degradation.

3.2. Performance of electrolyte-supported cells

Unlike anode-supported cells, electrolyte-supported button cells having an anode thickness of ~30 μm quickly degraded in the presence of AsH_3. Complete cell failure occurred within several hours in the presence of 10 ppm of AsH_3. Cell performance results following arsenic introduction to the coal gas are given in Fig. 5. Cells showed immediate degradation in the presence of arsenic followed by an even steeper loss in power output. Electrochemical impedance spectra showed a significant increase in both ohmic (high frequency or *x*-axis intercept) and electrodic (difference between low and high frequency *x*-axis intercepts) contributions to overall cell resistance, typical results of which are shown in Fig. 6. This behavior is consistent with nickel particle reaction and coalescence, which would affect ohmic losses, as well as poisoning of the active interface in these cells having a relatively thin anode and coarse microstructure, which would alter electrodic losses.

Conversion of nickel to form nickel arsenide phases and extensive product grain growth were apparent due to arsine exposure. Fig. 7 shows reaction progress for cells exposed to 0–10 ppm arsine

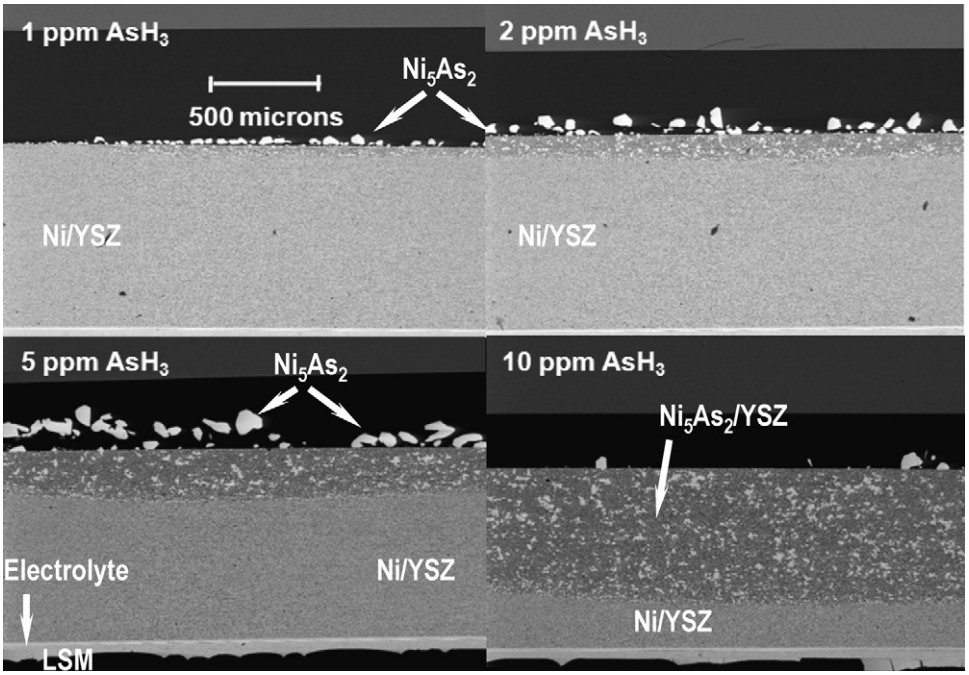

Fig. 3. SEM cross-section images of four Ni/YSZ anode-supported cells after 480 h exposure to coal gas containing 1, 2, 5, or 10 ppm AsH_3 at 800 °C. Reaction products on the surface and in the upper part of the anode support shown as light features are Ni_5As_2. Most of nickel arsenide reaction products spalled off from the surface of the sample exposed to 10 ppm AsH_3. The LSM cathode and dense YSZ electrolyte appear at the bottom of each image.

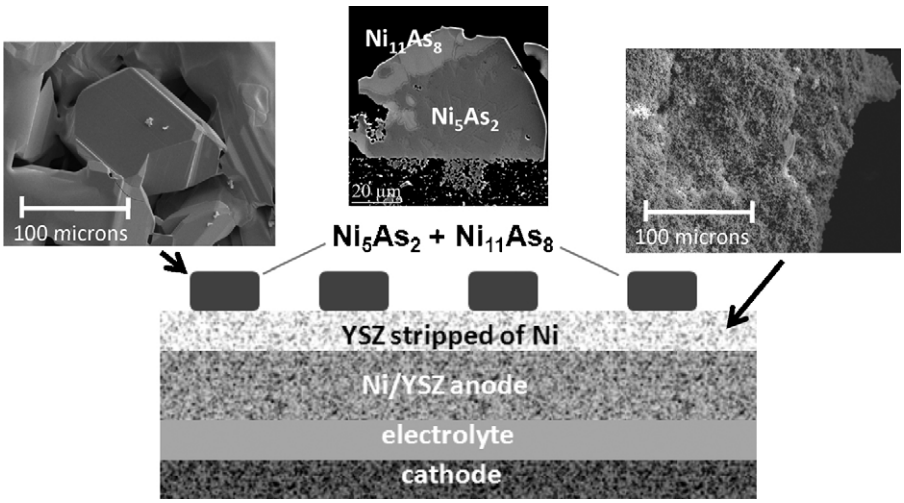

Fig. 4. Alteration of anode-supported cell following 480 h exposure to coal gas containing 10 ppm of AsH_3 at 700 °C.

for ~50 h in coal gas at 700 °C. Complete reaction of all nickel occurred within the test period for arsine concentrations equal to or greater than 5 ppm. The alteration phase Ni_5As_2 was the primary reaction product, identified by compositional analysis using EDS as well as by crystal structure using EBSD. At 700 °C and 10 ppm arsine, Ni_5As_2 was eventually converted to $Ni_{11}As_8$. The reaction products formed large grains on the surface of the anode, with nickel depleted from the anode, as observed for anode-supported cells. Grain growth increased with increased temperature, as expected. Results at 750 and 800 °C were very similar to those shown in Fig. 7. The product $Ni_{11}As_8$ was observed at 750 °C, though not within 50 h of exposure, whereas $Ni_{11}As_8$ was not observed at 800 °C for arsine concentrations of 10 ppm or smaller.

3.3. Coupon test results

Porous Ni/YSZ coupons were exposed to coal gas containing arsine in flow-through and flow-by configurations, aimed at

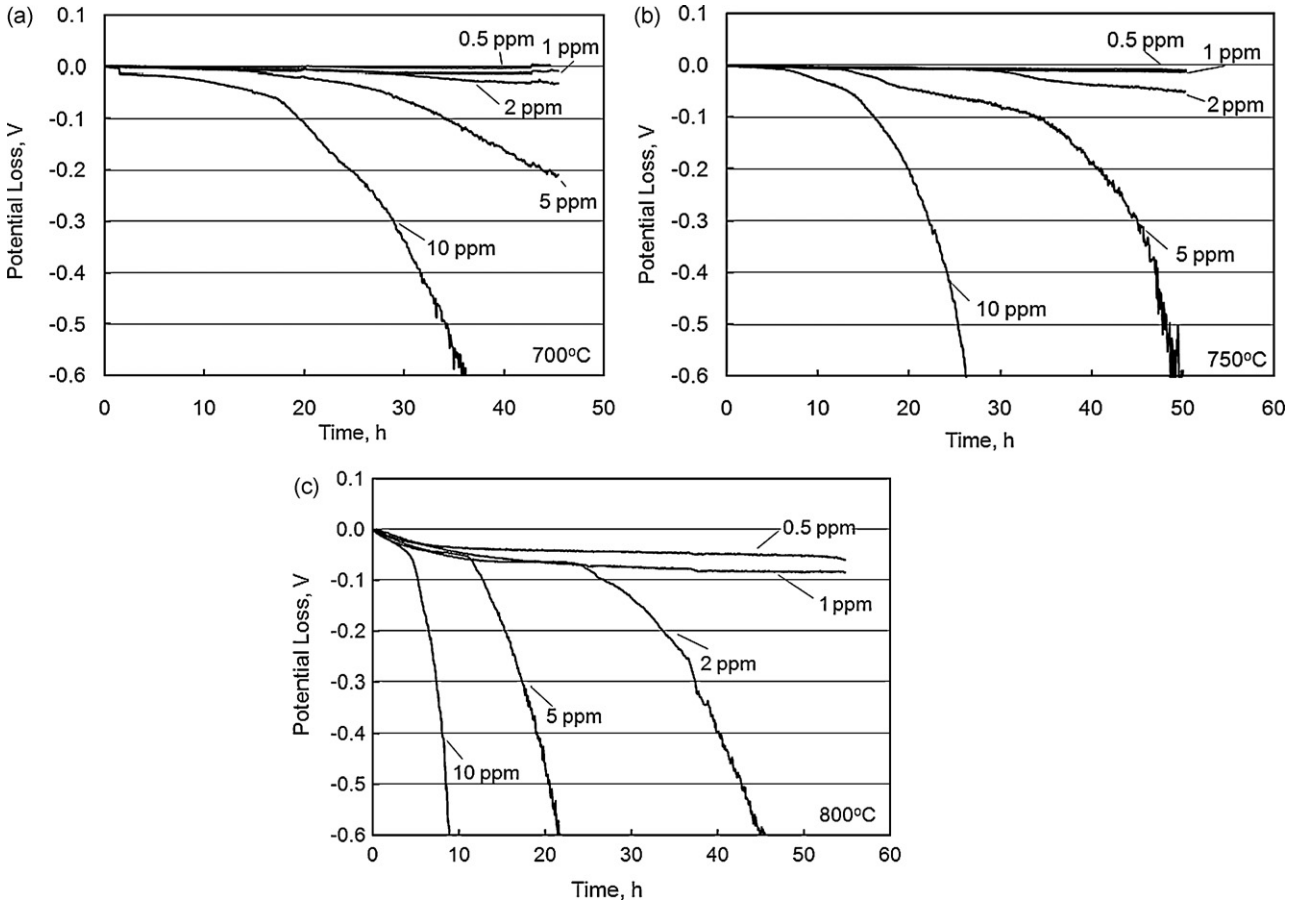

Fig. 5. Electrolyte-supported cell voltage losses at a constant current density of 0.05 A cm^{-2} after 0.5, 1, 2, 5, or 10 ppm of AsH_3 was added to coal gas at (a) 700 °C, (b) 750 °C, and (c) 800 °C.

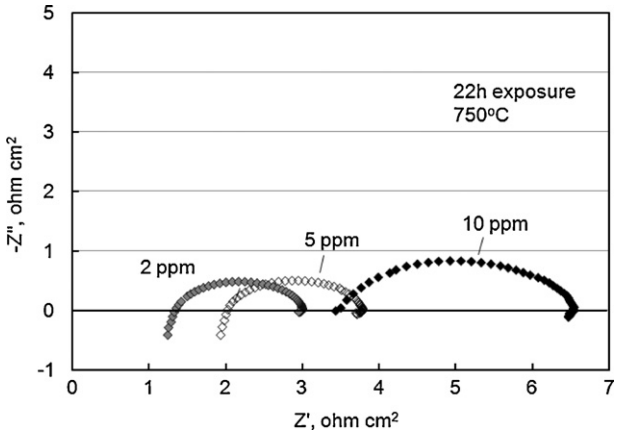

Fig. 6. Impedance spectra of the electrolyte-supported cells obtained at 750 °C at a bias current of 0.05 A cm^{-2} following 22 h exposure to coal gas containing the indicated arsenic concentrations.

providing additional qualitative information on the kinetics of arsenic–nickel reactions in a coal gas environment. In flow-through tests from 500 to 800 °C, all of the arsenic was captured in reaction with nickel. A very sharp boundary between reacted and unreacted portions of the coupon was present, very similar in appearance to results obtained for anode-supported cells shown in Fig. 3. Consistent with complete arsenic capture in this temperature range, no dependence of arsenic penetration depth into the coupon on temperature was established. Similar to the results of cell tests, large (10–20 μm in diameter) grains of nickel arsenide reaction products formed on the surface of the coupon, while nickel was depleted from reacted portions. Because no nickel current collector was present, all reaction products on the surface of the coupon originated from the Ni/YSZ composite. At 700 °C and higher, only Ni_5As_2 formation was observed, while at lower temperatures $Ni_{11}As_8$ was observed in addition. This product was predominant on the surface of the coupons at 500 and 600 °C.

Coupons were also tested in a flow-by arrangement, aimed at reproducing the configuration of a cell within a planar SOFC stack. As is shown in Fig. 8, arsenic was largely captured near the inlet of fuel gases in a band approximately 4 mm thick, demonstrating

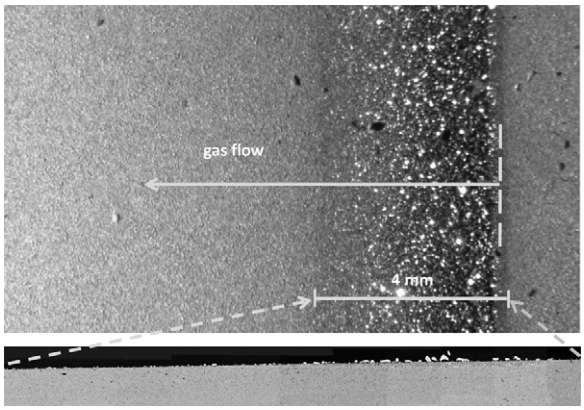

Fig. 8. Surface view of a porous Ni/YSZ coupon (top) and an SEM cross-sectional micrograph of a corresponding transformed area (bottom) following exposure to 2 ppm arsine in coal gas for 500 h at 700 °C. The cross-sectional micrograph at bottom corresponds to a 4 mm wide portion of the surface view at top, as indicated by dashed lines. The coupon was mounted in a test fixture intended to simulate a cell in a planar SOFC stack. Arsine was completely captured in a narrow band near the gas inlet to form Ni_5As_2 crystals appearing as bright features.

relatively fast reaction kinetics. SEM/EDS results revealed that large Ni_5As_2 crystals had formed at or in the vicinity of the gas inlet, while smaller Ni_5As_2 crystals were found up to 6 mm from the gas inlet. A cross-sectional SEM analysis also included in Fig. 8 showed that Ni_5As_2 had formed to a maximum depth of 50 μm within ~2 mm of the gas inlet. These results demonstrate that arsenic interactions with the nickel-based anode would not occur uniformly, but would be concentrated near the fuel gas inlet of an SOFC stack.

4. Discussion

4.1. Comparison of experimental phase analyses to calculated phase boundaries

Nickel and arsenic are known to form several intermetallic compounds: Ni–arsenic solid solution (Ni(ss)), Ni_5As_2, $Ni_{11}As_8$, NiAs, and $NiAs_2$ [19–22]. The maximum solubility of arsenic in nickel has been determined to be 4.5 at.% at the eutectic temperature of 897 °C.

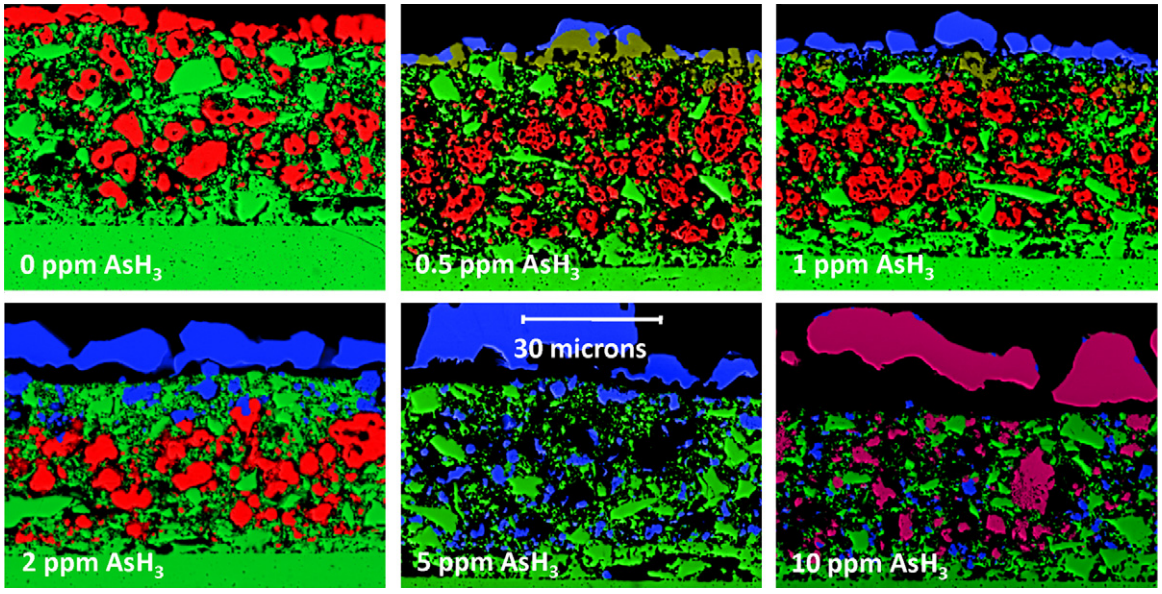

Fig. 7. Cross-sectional elemental maps showing arsenic penetration into the Ni/YSZ anode of electrolyte-supported cells after 50-h exposure to synthetic coal gas at 700 °C containing indicated arsine concentrations. Ni is red, Ni–As solid solution (low As) is dark yellow, Ni_5As_2 is blue, $Ni_{11}As_8$ is magenta, and YSZ is green. The dense YSZ electrolyte appears at the bottom of each image.

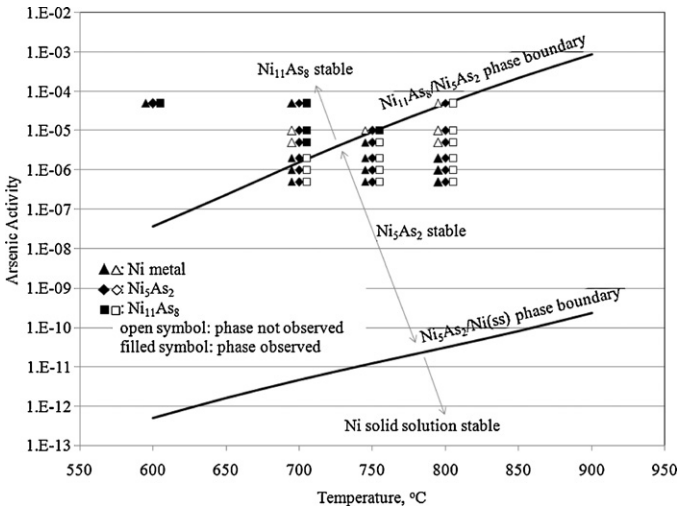

Fig. 9. Comparison of nickel alteration phases observed in cell and coupon tests with calculated phase boundaries. Arsenic activities corresponding to 0.5–10 ppm were employed in anode-supported and electrolyte-supported cell tests. An arsenic activity of 50 ppm was used in certain coupon tests, where coupons were only partially converted.

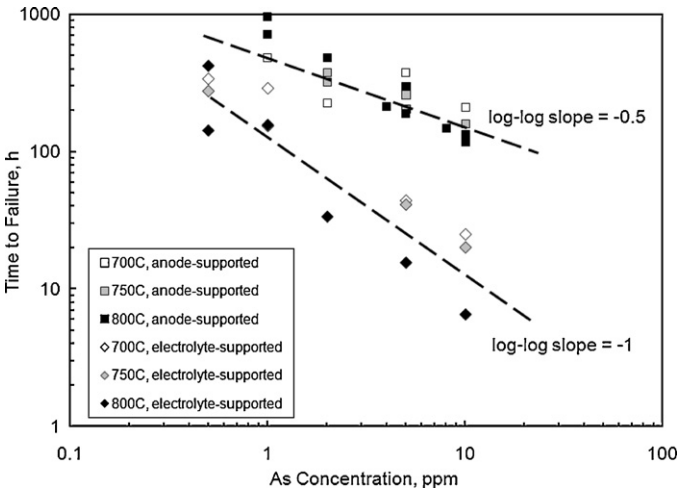

Fig. 10. Time to failure for electrolyte-supported and anode-supported button cells exposed to simulated coal gas with varying concentrations of arsenic. The criterion for failure is an increase of 0.2 V in polarization resistance.

A eutectic reaction occurs between Ni(ss) and Ni_5As_2 at 897 °C, whereas the compound Ni_5As_2 melts congruently at 998 °C. The phase $Ni_{11}As_8$ decomposes by peritectic reaction at 830 °C to form the solid solution NiAs and a liquid, whereas a eutectic reaction occurs between Ni_5As_2 and $Ni_{11}As_8$, with a low eutectic reaction temperature of 804 °C. The solid solution NiAs melts congruently at 970 °C. The phase $NiAs_2$ is not expected to form in coal gas with realistic arsenic concentrations.

Equilibrium calculations were performed to link arsenic concentrations in coal gas to the nickel–arsenic phase diagram using HSC Chemistry Version 6 and included thermodynamic data [23]. As is given in Fig. 9, the solid phase Ni_5As_2 is expected to be formed in coal gas over a broad temperature range for arsenic concentrations less than 1 ppb. This is consistent with observations made previously on nickel catalysts [13]. Arsenic concentrations in Fig. 9 represent the sum of all expected arsenic-containing species weighted by the number of arsenic atoms in each species, of which As(g), As_2(g), As_3(g), As_4(g), AsH(g), AsH_2(g), AsH_3(g), and AsO(g) were included in the calculations. Though introduced as AsH_3(g), the species As_2(g) is predicted to predominate in coal gas over a wide range of fuel utilization.

The solid phase Ni_5As_2 is expected to be converted to $Ni_{11}As_8$ at substantially higher arsenic activities, e.g. in $\geq\sim$5 ppm arsenic at 700 °C. Formation of the solid phase NiAs is predicted to occur only at considerably higher arsenic concentrations in coal gas than considered in this study, though small quantities have been reported to be produced at arsine concentrations as low as 0.1 ppm on fuel cell anodes [14]. Also included in Fig. 9 is a summary of conditions under which nickel arsenide phases were observed experimentally in button cell and coupon tests. Filled symbols indicate that the particular solid phase was experimentally identified at indicated temperatures and arsenic concentrations, whereas an open symbol indicates that the solid phase was not observed. Conditions required for the appearance of the phase $Ni_{11}As_8$ are reasonably consistent with the calculated boundary. It was not practical to probe minimum conditions needed to form Ni_5As_2, given that required arsenic concentrations are exceptionally low and that very long reaction times would be necessary to be able to observe product formation. It is important to recognize that equilibrium is most frequently not achieved in these tests, due to a combination of insufficient reaction time and insufficient arsenic supplied. As such, more nickel-containing phases are often present than is allowed by the Gibbs phase rule for a two-component system at constant pressure.

The formation of $Ni_{11}As_8$ would be undesirable, given that the temperature of the eutectic reaction of that phase with Ni_5As_2 is quite low (804 °C). The presence of a liquid phase would quickly result in cell failure due to rapid sintering and loss of mechanical strength. However, it is highly unlikely that conditions leading to $Ni_{11}As_8$ would ever exist in an SOFC power plant fueled by coal gas. First, the concentration of arsenic in coal gas is expected to be maintained well below the phase boundary for $Ni_{11}As_8$ through the use of absorbers and other cleanup options. Formation of Ni_5As_2 is possible, given the fact that the phase boundary corresponds to subparts per billion concentrations of arsenic in the temperature range of interest.

4.2. Degradation processes

The ultimate goal of this research is to establish acceptable concentrations of contaminants in coal gas intended to fuel large SOFC plants. Arsenic, because of its strong tendency to form alteration phases in reactions with nickel, is among the more important contaminants to be addressed. Experimentally determined times to failure for button cells versus contaminant concentration provide a basis for estimation of SOFC stack lifetimes operating on coal gas. Extrapolation of relatively short-term degradation results corresponding to high arsenic concentrations of course requires a thorough understanding of the mechanism of failure to predict lifetimes at much lower concentrations.

A summary of cell lifetimes in simulated coal gas containing varying concentrations of arsenic for electrolyte- and anode-supported button cells is given in Fig. 10. The criterion for cell failure is a somewhat arbitrary increase in polarization loss of 0.2 V attributable to arsenic exposure. In this study, cells were operated at constant current densities. Because cathode performance was quite stable, changes in cell polarization in the presence of arsenic in coal gas can be attributed solely to the anode. Times to failure electrolyte-supported cells generally followed a reaction order of −1 on gas-phase arsenic concentration (doubling of the arsenic concentration decreased the lifetime by a factor of 2), whereas times to failure of anode-supported cells followed approximately a −1/2 order dependence on arsenic concentration. Rates of degradation for neither electrolyte- or anode-supported cells showed any dependence on current density or fuel utilization, consistent

with the conclusion that strong interactions between nickel and arsenic occur, leading to essentially complete arsenic capture to exceptionally low concentrations in coal gas.

Electrolyte-supported cells, with a ~30 μm-thick Ni/YSZ anode and a relatively coarse microstructure, failed considerably more quickly for a given arsenic concentration than anode-supported cells, the latter of which have a substantially larger nickel inventory. From electrochemical impedance spectra shown in Fig. 6, it is apparent that increases in both the ohmic and electrodic contributions to electrolyte-supported cell losses had occurred as the cell degraded due to arsenic exposure. With poisoning of a portion of the active anode/electrolyte interface, apparent ohmic contributions also increased because only a fraction of the cell remained active. The temperature dependence of degradation was modest for electrolyte-supported cells: degradation rates at 800 °C were approximately double those measured at 700 and 750 °C. From phase equilibria considerations, reaction to form Ni_5As_2 is possible for arsenic concentrations in coal gas far lower than those used in this study. The kinetics of nickel–arsenic reactions occur sufficiently quickly that the anode is progressively converted from the outside surface to active interface (see Fig. 7). Significant performance losses did not occur for electrolyte-supported cells until the reaction front had approached the active interface. Given the approximately first-order dependence of lifetime on arsenic concentration shown in Fig. 10, the lifetime of electrolyte-supported cells can be straightforwardly estimated from matching the nickel inventory to arsenic concentration in coal gas, flow rate, and time of exposure.

For anode-supported cells, failure occurred well before arsenic had penetrated to the active anode/electrolyte interface. Failure of these cells occurred abruptly, as shown in Fig. 1, whereas there was little evidence of cell degradation prior to complete failure. The mode of failure clearly is related to loss of electrical connectivity within the anode support. Conversion of nickel to Ni_5As_2 was accompanied by extensive coalescence of the reaction products on the outer surface of the anode. The observation of a reaction order of approximately −1/2 for the arsenic concentration range of 1–10 ppm in Fig. 10 suggests that a diffusional process may be the rate-limiting step. That process is likely the diffusion of Ni_5As_2 from inside the anode support to the support surface followed by coalescence, leaving a YSZ layer devoid of electronically conductive material. Nickel arsenide phases are highly electronically conductive [18]. Had those products remained in place, no cell performance likely would have been observed within the time period of these tests. This reaction order of −1/2 should not extend indefinitely for anode-supported cells, of course. For very low arsenic concentrations, the time required to deliver the critical amount of arsenic needed to cause cell failure would be long compared to that for diffusional processes. As such, times to failure are expected to follow a reaction order of −1 for low arsenic concentrations, similar to the behavior of electrolyte-supported cells.

Estimates of SOFC stack lifetime in coal gas containing arsenic must take into account conditions under which present button cell tests were performed versus those likely to be employed in a planar stack. From an extrapolation of the results of Fig. 10 for electrolyte-supported button cells (reaction order of −1) to desired minimum 40,000 h SOFC stack lifetime [1–4], a maximum concentration of 1–10 ppb arsenic in coal gas can be estimated. However, gas flow rates in present button cell tests corresponded to ~15% fuel utilization if operated at 0.5 W cm^{-2} (0.7 V), whereas ~85% fuel utilization would be more typical for large-scale power generation with SOFC systems—roughly a difference of a factor of 5. Maximum acceptable arsenic concentration estimates should be increased by a similar factor, because higher fuel flow rates in current button cell tests correspond to greater net arsenic delivered to the cells and because virtually all arsenic in coal gas was captured by the nickel anode. The uniformity of arsenic uptake should also be considered. In tests with button cells, nickel arsenide reaction products were formed relatively uniformly across the anode surface. In coupon tests simulating the operation of a planar stack, however, arsenic was completely captured within a narrow band near the gas inlet (Fig. 8). Such behavior may be an advantage, as most of the planar cell and stack would not be subjected to arsenic exposure at realistic arsenic concentrations and flow rates. Removal of arsenic from coal gas to ~10 ppb levels is recommended to avoid such issues.

5. Summary and conclusions

Nickel/YSZ anode-supported and electrolyte-supported cells were tested in synthetic coal gas containing arsenic in concentrations of 0–10 ppm at 700–800 °C. Arsenic was found to interact strongly with nickel in the anode, leading to the formation of nickel–arsenic solid solution, Ni_5As_2 and $Ni_{11}As_8$, depending on temperature, arsenic concentration, flow rate and time. A sharply defined boundary was created between converted and unconverted portions of the anode. The appearance of nickel arsenide phases was in good agreement with calculated solid phase boundaries in coal gas. Rates of degradation showed no dependence on either current density or on fuel utilization.

The lifetime of anode- and electrolyte-supported cells showed different dependencies on arsenic concentration. For anode-supported cells, loss of electrical connectivity in the anode support was the principal mode of failure, as nickel was converted to nickel arsenide, which then migrated to the surface and formed large grains. Cell failure occurred well before the entire anode was converted to nickel arsenide. Until this occurred, there was typically very little electrochemical evidence of degradation. Time to failure followed a reciprocal square root of arsenic partial pressure dependence, consistent with a diffusion-based rate-limiting step for arsenic exposure in the 1–10 ppm range. Failure occurred more quickly with electrolyte-supported cells, which have a substantially smaller nickel inventory. For these cells, times to failure varied linearly with the reciprocal arsenic concentrations in coal gas, attributed to arsenic at least partially reaching the active anode/electrolyte interface. Though large grains of reaction product formed, electrical connectivity within the anode did not appear to be lost within the time scale of these tests.

Arsenic is expected to be non-uniformly captured by the anode of an SOFC, concentrating near the fuel gas inlet. Though a small portion of the cell may cease to function depending on arsenic concentration and flow rate, operation of the remainder of the cell is not expected to be affected. Arsenic concentrations of ~10 ppb or less are estimated to result in acceptable rates of fuel cell degradation, less than projected concentrations based on current warm-gas cleanup strategies [5] but certainly achievable.

Acknowledgements

The authors appreciate SEM analyses performed by AL Schemer-Kohrn and SEM sample preparation by CE Chamberlin. Financial support from the U.S. Department of Energy, Office of Fossil Energy, National Energy Technology Laboratory as part of the Solid State Energy Conversion Alliance (SECA) Coal-Based Systems Core Research Program (Dr. Paul Tortora, contract manager) is gratefully acknowledged. Pacific Northwest National Laboratory is operated by Battelle for the U.S. Department of Energy under Contract AC06-76RLO 1830.

References

[1] U.S. Dept. of Energy Office of Fossil Energy, FutureGen: Integrated Hydrogen, Electric Power Production and Carbon Sequestration Research Initiative, March 2004.

[2] M.C. Williams, J.P. Strakey, W.A. Surdoval, Int. J. Appl. Ceram. Technol. 2 (2005) 295.
[3] M.C. Williams, J.P. Strakey, W.A. Surdoval, J. Power Sources 143 (2005) 191.
[4] M.C. Williams, J.P. Strakey, W.A. Surdoval, L.C. Wilson, Solid State Ionics 177 (2006) 2039.
[5] J.P. Trembly, R.S. Gemmen, D.J. Bayless, J. Power Sources 163 (2007) 986.
[6] F.N. Cayan, M.J. Zhi, S.R. Pakalapati, I. Celik, N.Q. Wu, R. Gemmen, J. Power Sources 185 (2008) 595.
[7] S.A. Benson, T.A. Erickson, C.J. Zygarlicke, C.A. O'Keefe, K.A. Katrinak, S.E. Allen, D.J. Hassett, W.B. Hauserman, N.T. Holcombe, Proceedings of the Advanced Coal-Fred Power Systems Review Meeting, Morgantown, WV, USA, July 16–18, 1996.
[8] A.E. Pigeaud, J.J. Helbe, Proceedings of the Coal-Fired Power Systems 94—Advances in IGCC, Morgantown, WV, USA, June 21–23, 1994.
[9] D.E. Ridler, M.V. Twigg, in: M.V. Twigg (Ed.), Catalyst Handbook, Manson Publishing, London, UK, 1997, p. 225.
[10] C.F. Ng, Y.J. Chang, Appl. Catal. 70 (1991) 213.
[11] C.F. Ng, H. Ye, L. She, H. Chen, S.Y. Lai, Appl. Catal. A 171 (1998) 293.
[12] R. Quinn, T. Mebrahtu, T.A. Dahl, F.A. Lucrezi, B.A. Toseland, Appl. Catal. A 264 (2004) 103.
[13] B. Nielsen, J. Villadsen, Appl. Catal. 11 (1984) 123.
[14] J.P. Trembly, R.S. Gemmen, D.J. Bayless, J. Power Sources 171 (2007) 818.
[15] O.A. Marina, L.R. Pederson, D.J. Edwards, C.A. Coyle, J.W. Templeton, M.H. Engelhard, Z. Zhu, ECS Trans. 11 (2008) 63.
[16] O.A. Marina, L.R. Pederson, G.W. Coffey, C.A. Coyle, C.D. Cramer, D.J. Edwards, 9th Annual Solid State Energy Conversion Alliance Workshop, Pittsburgh, PA, USA, August 5–7, 2008.
[17] G. Krishnan, 9th Annual Solid State Energy Conversion Alliance Workshop, Pittsburgh, PA, USA, August 5–7, 2008.
[18] D.R. Lide, Handbook of Chemistry and Physics, CRC Press, Boca Raton, FL, USA, 1993.
[19] T.B. Massalski, Binary Alloy Phase Diagrams, 2nd ed. with Updates, H. Okamoto, editor, ASM International, National Institute of Science and Technology, Materials Park, Ohio, 44073, 1996.
[20] M. El-Boragy, M. Ellner, B. Predel, Zeitschrift Fur Metallkunde 74 (1983) 545.
[21] R.D. Heyding, L.D. Calvert, J. Canadian, Chemistry-Revue Canadienne De Chimie 35 (1957) 1205.
[22] A. Kjekshus, K.E. Skaug, Acta Chem. Scand. 27 (1973) 582.
[23] A. Roine, HSC Chemistry 6, version 6.12, Outokumpu Research Oy, Pori, Finland, 2007, www.outotec.com.